A Journal of the Gesellschaft Deutscher Chemiker

Angewandte International Edition GDCh Chemie

www.angewandte.org

Accepted Article

Title: Control of Luminescence via Tuning of Crystal Symmetry and Local Structure in Mn4+-Activated Narrow Band Fluoride Phosphors

Authors: Mu-Huai Fang, Wei-Lun Wu, Ye Jin, Tadeusz Lesniewski, Sebastian Mahlik, Marek Grinberg, Mikhail G. Brik, Alok M. Srivastava, Chang-Yang Chiang, Wuzong Zhou, Donghyuk Jeong, Sun Hee Kim, Grzegorz Leniec, Slawomir M. Kaczmarek, Hwo-Shuenn Sheu, and Ru-Shi Liu

To be cited as: *Angew. Chem. Int. Ed.* 10.1002/anie.201708814
Angew. Chem. 10.1002/ange.201708814

Link to VoR: http://dx.doi.org/10.1002/anie.201708814
http://dx.doi.org/10.1002/ange.201708814

WILEY-VCH

Narrow-band-emitting red phosphor DOI: 10.1002/anie.201((will be filled in by the editorial staff))

Control of Luminescence via Tuning of Crystal Symmetry and Local Structure in Mn^{4+}-Activated Narrow Band Fluoride Phosphors

Mu-Huai Fang,[⊥] Wei-Lun Wu,[⊥] Ye Jin, Tadeusz Lesniewski, Sebastian Mahlik, Marek Grinberg, Mikhail G. Brik, Alok M. Srivastava, Chang-Yang Chiang, Wuzong Zhou, Donghyuk Jeong, Sun Hee Kim, Grzegorz Leniec, Slawomir M. Kaczmarek, Hwo-Shuenn Sheu, and Ru-Shi Liu[*]

Abstract: *Manganese (Mn^{4+})-doped fluoride phosphors have been widely used in wide-gamut backlighting devices because of their extremely narrow emission band. In this study, solid solutions of $Na_2(Si_xGe_{1-x})F_6:Mn^{4+}$ and $Na_2(Ge_yTi_{1-y})F_6:Mn^{4+}$ have been successfully synthesized to elucidate the behavior of zero-phonon line (ZPL) in different structures because of the sensitivity of ZPL intensity to the local coordinated environment. The structures of the products are examined by X-ray diffraction and Rietveld refinement. The ratio between ZPL and the highest emission intensity υ_6 phonon sideband exhibits a strong relationship with luminescent decay rate. First-principles calculations are conducted to model the variation in the structural and electronic properties of the prepared solid solutions as a function of the composition. The calculated results are consistent with the experimentally determined structural parameters. To compensate for the limitations of Rietveld refinement, electron paramagnetic resonance and high-resolution steady-state emission spectra are used to prove the diverse local environment for Mn^{4+} in the structure. Finally, the spectral luminous efficacy of radiation (LER) is used to reveal the important role of ZPL in practical application.*

[*] Mr. Mu-Huai Fang,[⊥] Mr. Wei-Lun Wu,[⊥] Prof. Dr. Ye Jin, and Prof. Dr. Ru-Shi Liu*
Department of Chemistry
National Taiwan University
Taipei,Taiwan 106
Tel: (+) 886-2369-3121
E-mail: rsliu@ntu.edu.tw
⊥ Mu-Huai Fang and Wei-Lun Wu contributed equally to this work.

Prof. Dr. Ru-Shi Liu
Department of Mechanical Engineering and Graduate Institute of Manufacturing Technology, National Taipei University of Technology, Taipei 106, Taiwan

Prof. Dr. Ye Jin
School of Science, Chongqing University of Technology, Chongqing 400054, China

Mr. Tadeusz Lesniewski, Dr. Sebastian Mahlik, Prof. Dr. Marek Grinberg
Institute of Experimental Physics, Faculty of Mathematics, Physics and Informatics, University of Gdańsk, Gdansk, Wita Stwosza 57, 80-308 Gdansk, Poland

Prof. Dr. Mikhail G. Brik
College of Sciences, Chongqing University of Posts and Telecommunications, Chongqing 400065, China Institute of Physics, University of Tartu, Tartu 50411, Estonia
Institute of Physics, Jan Dlugosz University, Czestochowa PL-42200, Poland

Dr. Alok M. Srivastava
GE Global Research, One Research Circle, Niskayuna, NY 12309, USA

Dr. Chang-Yang Chiang and Prof. Dr. Wuzong Zhou
EaStCHEM, School of Chemistry, University of St Andrews, St Andrews, KY16 9ST, United Kingdom

Dr. Donghyuk Jeong and Prof. Dr. Sun Hee Kim
Western Seoul Center, Korea Basic Science Institute, University-Industry Cooperation Building, Seoul, 120-140, Korea

Dr. Grzegorz Leniec, Prof.Dr. Slamowir M. Kaczmarek, Institute of Physics, Department of Mechanical Engineering and Mechatronics, West Pomeranian University of Technology Szczecin, al. Piastow 48, 70-311 Szczecin, Poland

Dr. Hwo-Shuenn Sheu
National Synchrotron Radiation Research Center, Hsinchu 300, Taiwan

Supporting information for this article is available on the WWW under http://www.angewandte.org or from the author

The recent development of high-quality backlighting systems, such as 8K television or wide-color gamut mobile phone, has attracted much attention.[1-3] Narrow emission bandwidth phosphors should be developed to realize these high-quality systems. Among all colors, red photon generators are the most important materials to realize low color temperature and warm light in devices based on light emitting-diodes (LEDs). Traditional red phosphors, such as $MAlSiN_3$ (M = Ca and Sr), are not suitable for attaining high spectral luminosity, because the broad emission of these materials makes a poor match with the eye sensitivity curve (emission has intensity beyond 650 nm).[4] The sharp line emission of Mn^{4+}-activated fluoride phosphors are promising because of their zero waste photon ratios. The emission consists of narrow lines emission between 600–650 nm.[5-7] Furthermore, the phosphor does not absorb the emission of the $Y_3Al_5O_{12}:Ce^{3+}$ (YAG) phosphor in an LED device.[8] The luminescence of Mn^{4+}in solids is characterized by the zero-phonon line (ZPL) ($^2E \rightarrow {}^4A_2$) and associated sidebands (Stokes and anti-Stokes vibronic bands). The Mn^{4+} ZPL intensities in certain fluorides and oxidic phosphors have been reported.[9-11] The intensity of the ZPL, which corresponds to the emission without the participation of any phonons, is dependent on the host lattice. Compared with five phonon sidebands (PSs), ZPL is much more sensitive to the local coordinated environment. Thus, the ZPL has very low intensity in the most popular fluoride phosphors, such as $K_2SiF_6:Mn^{4+}$ and $K_2TiF_6:Mn^{4+}$.[12-14] Nevertheless, most of the studies on Mn^{4+} doped fluoride phosphors have focused on the synthesis of new compounds or different synthesis methods. While the behavior of ZPL is rarely studied deeply and systematically, and the correlation between the local coordination environment and luminescent behavior remains obscure.

In this study, the variation in ZPL intensity is examined in a series of compositions within the solid solutions of $Na_2(Si_xGe_{1-x})F_6:Mn^{4+}$ and $Na_2(Ge_yTi_{1-y})F_6:Mn^{4+}$. The dependence of ZPL intensity and associated PS on the local structure is analyzed by electron paramagnetic resonance (EPR), decay rate, and high-resolution steady-state emission. Furthermore, the luminous efficacy of radiation (LER; brightness) is used to reveal the important role of ZPL in practical applications. The results provide new insights for developing high-performance fluoride phosphor and realization of

10.1002/anie.201708814

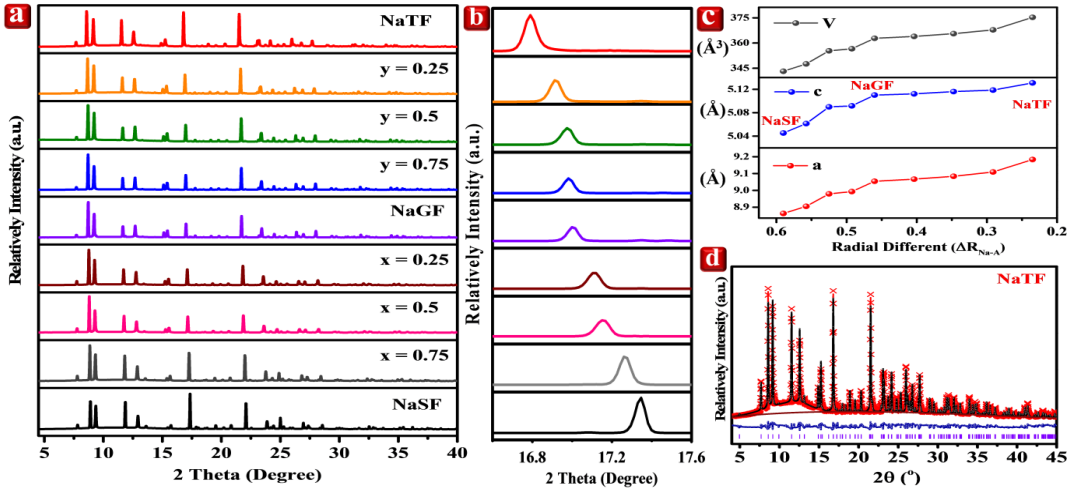

Figure 1. (a) Variations in XRD patterns with corresponding x and y values in $Na_2(Si_xGe_{1-x})F_6:Mn^{4+}$ and $Na_2(Ge_yTi_{1-y})F_6:Mn^{4+}$. (b) Peak shift during the variation of x and y. (c) Lattice parameters of Rietveld refinement. (d) Rietveld refinement XRD spectrum

some properties of ZPL. X-ray diffraction (XRD) patterns of $Na_2(Si_xGe_{1-x})F_6:Mn^{4+}$ and $Na_2(Ge_yTi_{1-y})F_6:Mn^{4+}$ were measured to analyze the structure of the solid solution (Figure 1a). Na_2GeF_6 (NaGF) and Na_2SiF_6 (NaSF) crystallize in the trigonal structure, space group P321, whereas Na_2TiF_6 (NaTF) has a triclinic structure with the space group P1.

In the structure, Mn^{4+} ions substitute at the Si^{4+}, Ge^{4+}, and Ti^{4+} positions forming octahedral MnF_6^{2-} moieties. Rietveld refinement is also conducted to show more details of the as-prepared samples (Figures 1d and S1). All χ^2, R_{wp}, and R_p values indicate good refinement (Table S1). The lattice parameters increase smoothly, and this characteristic is related to the ionic size (Figure 1c). The structural and electronic properties of the solid solutions in the whole range of cation concentrations were calculated using the CASTEP module of Materials Studio. Figure S2 shows the linear variation of the calculated lattice constants with composition and there is good agreement with the corresponding experimental data. The diffraction peaks shift to lower angles because of the larger ionic size of Ti^{4+}. Moreover, no additional peaks are found (Figure 1b), indicating the absence of secondary phases, such as NaSF, NaGF, or NaTF, and random distribution of Si/Ge and Ge/Ti in the $Na_2(Si_xGe_{1-x})F_6:Mn^{4+}$ and $Na_2(Ge_yTi_{1-y})F_6:Mn^4$ solid solutions. The practical chemical composition of the samples is measured by inductively coupled plasma optical emission spectrometry (ICP-OES) as shown in Table S2. Transmission electron microscopy (TEM) and selected area electron diffraction (SAED) were performed to further analyze the structure and crystallinity of the samples (Figure S3). The diffraction pattern shows good crystallinity with no clear indications of any superstructures. The *d*-spacing values calculated from the SAED pattern are very close to the Rietveld refinement results, which also proves the accuracy of the refinement. In addition, the local structure of Si^{4+}, Ge^{4+}, and Ti^{4+} obtained from Rietveld refinement is not absolutely the same as the local structure of Mn^{4+}. The relative low concentration of Mn^{4+} does not allow the assessment of the local MnF_6^{2-} coordination from Rietveld refinement.

The photoluminescence (PL) and photoluminescence excitation (PLE) spectra are measured to investigate the luminescent properties (Figure 2a and 2b). The excitation transitions are the spin-allowed $^4A_2 \rightarrow {}^4T_2$ (longer wavelength) and $^4A_2 \rightarrow {}^4T_1$ (shorter wavelength), the energy of which is strongly affected by the crystal field. In our case, no apparent changes in shape and position were observed in the excitation spectra. Thus, we assume that the strengths of the crystal fields in these systems are quite similar.

However, the emission spectra are dominated by the spin-forbidden $^2E \rightarrow {}^4A_2$ transition. Although the emission transition energy is much less sensitive to the strength of the crystal field compared with the excitation transitions, the ZPL intensity is sensitive to the distortion in the MnF_6^{2-} moieties. More specifically, the occurrence of ZPL is a result of static symmetry distortions that lift the inversion symmetry of the MnF_6^{2-} moiety. Such distortion causes an admixture of odd parity components to even parity ^2E and $^4A_2$ wavefunctions, thus lifting the Laporte selection rule that forbids dipole transitions between states of the same parity.[15]

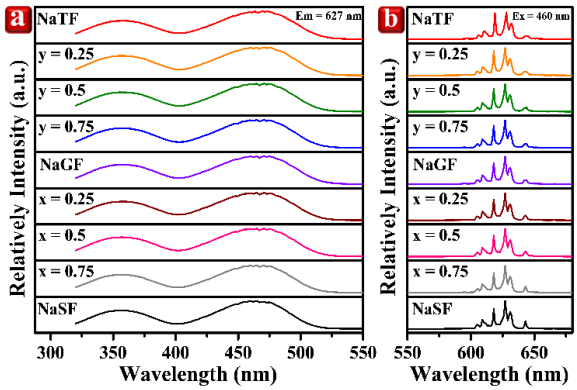

Figure 2. (a) Excitation and (b) emission spectra of $Na_2(Si_xGe_{1-x})F_6:Mn^{4+}$ and $Na_2(Ge_yTi_{1-y})F_6:Mn^{4+}$

The most straightforward way to assess distortions within the MnF_6^{2-} moieties is to determine the ZPL emission intensity (at approximately 617 nm) as a function of the F-Mn-F bond angles and the crystal structure. The other lines in the emission spectrum are assigned to the following PSs: υ_3 (t_{1u} stretching), υ_4 (t_{1u} bending),and υ_6 (t_{2u} bending) vibration mode. The ZPL intensity increases from NaSF through NaGF to NaTF. The ZPL intensity increases with decreasing symmetry of the emitting center. In NaSF and NaTF, two Si and three Ti sites are suitable for the Mn^{4+} ions. The Si1 site has nearly perfect octahedral symmetry, in which the distances of all six "central ion–fluorine" are equal, and the angles only slightly (by 1°–2°) differ from a perfect octahedron. However, the Si2 site in NaSF and all three sites in NaTF have considerably lower symmetry (see Supporting Information). The comparison of the F-central ion–F angles (Figures S4–S7) shows that the deviations from the ideal octahedron are much more pronounced in the NaTF crystal, which eventually explains the enhancement of the ZPL in this material.

10.1002/anie.201708814

The ZPL/υ6 (630 nm) intensity ratio (denoted as ZPL/υ6) is probed to systematically analyze the behavior of ZPL. First, the decay curve is measured to elucidate the relationship between the ZPL/υ_6 and lifetime (Figure S8). The reciprocal value of the calculated fluorescence lifetime is the decay rate. Figure 3 shows that the decay rate behaves similarly to the changes in the ZPL/υ_6 ratio. Moreover, the slopes for the trend of ZPL/υ_6 are much larger from NaGF to NaTF compared with that from NaSF to NaGF. This behavior can be explained on the basis of structural differences. NaSF and NaGF belong to the P321 trigonal system, which is more symmetrical than NaTF. Therefore, changes in the ZPL/υ_6 between NaSF and NaGF are small. The crystal structure of NaTF is P1 (pseudo) triclinic system, which is a low-symmetry space group. Thus, the ZPL/υ_6 value increases more rapidly when the space group changes to a lower symmetry.

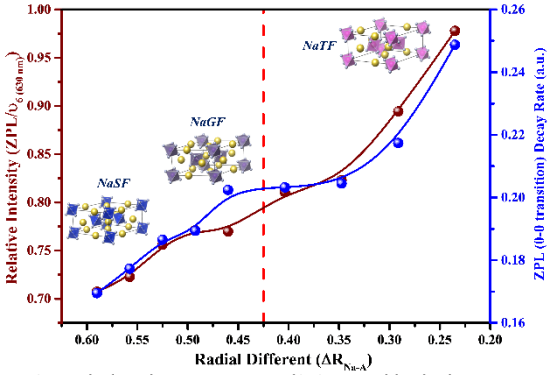

Figure 3. Relation between ZPL (0-0 transition) decay rate and relative intensity of ZPL/υ_6.

The low temperature (10 K) emission spectra of NaSF, NaGF, and NaTF were recorded from time-resolved emission spectroscopy (TRES) measurement to demonstrate the effect of the site distribution. The emission streaks over 10 ms time windows were integrated (Figure 4). Blue curves in Figure 4 present the emission spectra under blue light excitation (440 nm), in which the excitation of the ^2E state is mediated by the $^4T_2$ state. For every sample under this excitation, the decay time of ZPL is different from that of the PSs. Thus, multiple Mn^{4+}centers with different ZPL-to-PS intensity ratios (Figures S9 and S10) is suggested, because for the individual single site the lifetime from the vibronic sidebands should be the same as that of the ZPL.

The multiple Mn^{4+} site occupation is further confirmed via TRES measurements performed under direct resonant excitation of the ^2E state (616.7 nm) of each sample (Figure 4). Such excitation should selectively excite the Mn^{4+}centers with stronger (and thus more probable) ZPL transition, whereas excitation through the $^4T_2$ state is not selective and populates each site with equal probability. The use of time-resolved method is crucial to separate the initial excitation pulse from the consecutive ZPL luminescence occurring at the same wavelength. The emission spectra under ZPL resonant excitation are represented by red lines in Figure 4. The obtained emission spectra have much higher ZPL intensities with respect to PS compared with those excited by blue light. Additionally, the discrepancy between the ZPL and PS decay times is greatly reduced (Figures S9 and S10), which confirms that the Mn^{4+} sites with low ZPL-to-PS ratio are not excited efficiently. These results confirm that the Mn^{4+} in $Na_2(Si,Ge,Ti)F_6:Mn^{4+}$ series are not equivalent, and Mn^{4+}centers with higher and lower ZPL/υ_6 intensity ratios exist.

A more straightforward or more sensitive method is explored to evaluate the local coordination environment of MnF_6^{2-} in our phosphors. This information cannot be obtained from the Rietveld refinement, which could only detect the coordination environment of AF_6^{2-} (A = Si, Ge, and Ti), not for the impurity MnF_6^{2-} moieties. When the MnF_6^{2-} ion is doped into the AF_6^{2-}, local distortion is expected due to differences between the ionic radii of the host cation and the impurity. EPR is used to determine the degree of distortion

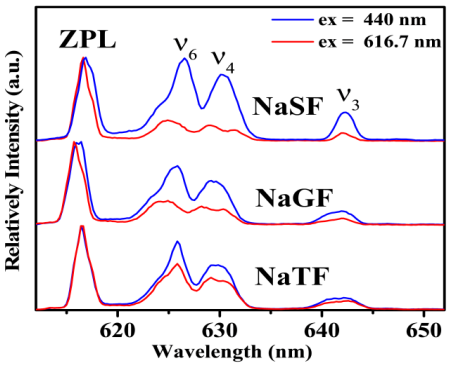

Figure 4. Luminescence spectra of NaSF, NaGF, and NaTF obtained under excitation 440 nm (blue curves) and under 616.7 nm (red curves) at the temperature of 10 K.

(Figure S11). In the analyzed powder samples the EPR signal is derived from the paramagnetic Mn^{4+} ion. It is characterized by a fine structure (S = 3/2) and a hyperfine structure (I = 5/2, 100%). The powder EPR spectrum of the NaSF sample consists of 4 signals with 6 characteristic peaks centered at different positions of the magnetic field (B ~ 220, 290, 340, 400 mT). Based on the positions, one can determine the local symmetry of Mn^{4+} ions. The strongest signal is centered at B ~ 340 mT and is attributed to isolated Mn^{4+} ions at relatively high local symmetry. The remaining EPR signals have much lower intensity. They are assigned to isolated Mn^{4+} ions at low local symmetry. In the NaSF sample we have two magnetically different positions of Mn^{4+} ions. Based on the analysis of the integral intensity of EPR signal, it can be concluded that much more ions exist as isolated Mn^{4+} ions at relatively higher than at lower symmetry (Mn^{4+}(Low Symmetry) = 0.19). EPR spectrum recorded for the NaGF sample is similar to the above analyzed NaSF one. Two magnetically different Mn^{4+} centers can be recognized. One of the centers at higher symmetry, the other one at lower symmetry (Mn^{4+}(LS) = 0.37). The calculation of the integrated intensity of EPR signal indicates that the number of Mn^{4+} centers in the higher symmetry decreases, and increases in the lower symmetry as compared to the NaSF. In the NaTF sample one can observe many EPR signals with hyperfine structure of Mn^{4+} ion. The EPR spectrum indicates at least two magnetically different positions of Mn^{4+} ions. The number of manganese centers at high and low symmetry is comparable (Mn^{4+}(LS) ~ 0.46). For NaSF, NaGF and NaTF compounds the integral intensity of the EPR signal increases, reaches the maximum value for NaGF and then decreases, respectively. The behavior of the integral intensity of the EPR signal is similar to the luminous efficacy of radiations (Figure 5). The ratio of low and high symmetry Mn^{4+} ions increases and reaches a maximum value for NaTF. The intensity of the ZPL correlates with the amount of Mn^{4+} ions at low symmetry. Also, high-resolution steady-state emission spectra are measured at 10 K under excitation at 442 nm to explore for another evidence of multi-sites or multi-environment in $Na_2(Si,Ge,Ti)F_6:Mn^{4+}$ (Figure S12). The obtained fine structure of ZPL and PS is much more complex than expected (Rietveld refinement), and up to four lines related to the ZPL transition can be distinguished. These data provide strong evidence for multiple Mn^{4+} sites in the crystalline lattice of these fluorides. Our analysis of the experimental data provides insights into the local-coordinated environment of Mn^{4+} and shows that probing the region of ZPL provides an understanding of structure–property relationships.

After associating the ZPL properties with the structure, the practical benefits of the ZPL intensity are demonstrated. The chief difference between the fluoride phosphors with strong and weak ZPL intensities are their spectral luminous efficacy of radiations (LERs) and color rendering indices (CRIs). In our previous study on $Rb_2GeF_6:Mn^{4+}$ phosphor, we demonstrated that the ZPL will help increase the CRI and R_9value according to the white LED package spectrum. In the current study, we demonstrate the theoretical effect of varying the ZPL intensity. The LER provides the theoretical

maximum luminescent efficiency for a given luminescent spectrum with the unit of lumen per watt (usually denoted as lm/W_{opt}). The LER could be directly calculated by the quotient of luminous flux by the corresponding radiant flux, as follows:

$$K = \frac{\Phi_v}{\Phi_e} = \frac{\int_0^\infty K(\lambda)\Phi_{e,\lambda}\,d\lambda}{\int_0^\infty \Phi_{e,\lambda}\,d\lambda} \quad (1)$$

$$\Phi_v = 683.002\ lm/W \cdot \int_0^\infty \bar{y}(\lambda)\Phi_{e,\lambda}\,d\lambda \quad (2)$$

where Φ_v is the luminous flux, Φ_e is the radiant flux, $\bar{y}$ is the eye sensitivity curve, and $\Phi_{e,\lambda}$ is the given spectrum. The maximum value of $K(\lambda)$ for photopic vision is 683.002 lm/W. Therefore, the LER values can be calculated from the luminescent spectrum. The LER value increases from NaSF and reaches the maximum value of 235 lm/W_{opt} with the composition of $Na_2Ge_{0.75}Ti_{0.25}F_6:Mn^{4+}$(Figure 5). Surprisingly, the LER value starts to decrease afterward and does not follow the trend of the ZPL intensity. This phenomenon is due to the fact that the intensity of the anti-Stoke peaks, υ_4 and υ_6, also slightly decrease and this cause the net LER value to decrease. Moreover, the performance of the $Rb_2GeF_6:Mn^{4+}$ phosphor, which also possesses high ZPL intensity, is investigated. Interestingly, the calculated value is only 205 lm/W_{opt}. The reason for the unexpectedly low ZPL in this case is due to the higher red-shift of the emission wavelength of $Rb_2SiF_6:Mn^{4+}$than those of the solid solution compounds, resulting in lower calculated LER. Therefore, these results suggest that, in addition to the intensity of ZPL, the effect of the total emission spectrum, which includes the relative intensity of the PS and luminescent wavelength from other peaks, should be considered. The LER values of $Na_2(Si_xGe_{1-x})F_6:Mn^{4+}$ and $Na_2(Ge_yTi_{1-y})F_6:Mn^{4+}$ are compared with those of the commercial fluoride phosphor $K_2SiF_6:Mn^{4+}$. The LER value of $K_2SiF_6:Mn^{4+}$ is only 200 lm/W_{opt}, which is much lower than those of $Na_2(Si_xGe_{1-x})F_6:Mn^{4+}$ and $Na_2(Ge_yTi_{1-y})F_6:Mn^{4+}$. This result is only one aspect that is important for practical application. The quantum efficiency and reliability of any new phopshor system should be evaluated to determine the performance in actual devices. However, although the luminescent intensity of $Na_2(Si_xGe_{1-x})F_6:Mn^{4+}$ and $Na_2(Ge_yTi_{1-y})F_6:Mn^{4+}$ is lower than that of commercial fluoride phosphor, such as $K_2SiF_6:Mn^{4+}$ (Figure S13), the LER value is attractive to further optimize this phosphor system.

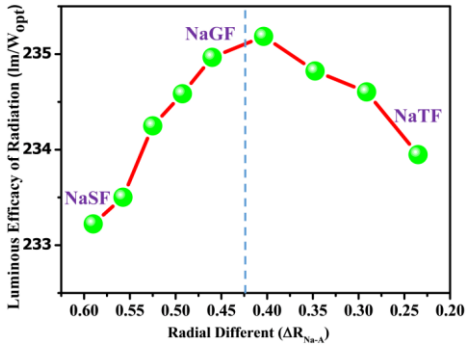

Figure 5. Luminous efficacy of radiation value of the spectrum of a solid solution of NaTF, NaGF, and NaSF

In summary, a series of solid solutions of $Na_2(Si_xGe_{1-x})F_6:Mn^{4+}$ and $Na_2(Ge_yTi_{1-y})F_6:Mn^{4+}$ have been successfully synthesized by the co-precipitation method. All as-prepared samples have pure phase as determined by Rietveld refinement. The PL spectra show that the ZPL intensity continuously increases from NaSF to NaGF and NaTF. Moreover, ZPL decay rate shows similar trend with ZPL/υ_6 ratio. The rate of increase in ZPL/υ_6 intensity is much faster than that from NaGF to NaTF compared with that from NaSF to NaGF. This phenomenon is connected with the structural change from trigonal system to triclinic system. The high-resolution steady-state emission spectra show the diverse local environment for the Mn^{4+} ion. EPR is measured to realize the real local coordination environment of MnF_6^{2-} cluster. EPR studies indicate the presence of at least two different positions of Mn^{4+} ions at high and low local symmetry. The result also shows that the coordination environment in NaTF is much more complex than in NaSF and NaGF. Finally, the LER values are calculated from their luminescent spectrum, which reaches a maximum value of approximately 235 lm/W_{opt} for $Na_2Ge_{0.75}Ti_{0.25}F_6:Mn^{4+}$ and starts to decrease afterward. These results show that the LER estimations are dependent on ZPL and the intensity of PS. Although the real luminescent intensity of $Na_2(Si_xGe_{1-x})F_6:Mn^{4+}$ and $Na_2(Ge_yTi_{1-y})F_6:Mn^{4+}$ is lower than the commercial fluoride phosphor, $K_2SiF_6:Mn^{4+}$, the LER values indicate the higher potential with proper optimization.

Analyzing the ZPL could be beneficial in the exploration of structure-property relationships. A correlation between the ZPL intensity and degree of deviation of the MnF_6 octahedral clusters from the ideal octahedral symmetry is observed. These techniques are valid for all fluoride phosphors, in which the ZPL can be properly identified. Finally, the higher LER for the fluoride phosphors with stronger ZPL intensity has facilitated the study for future narrow-emission red phosphor.

Experimental Section

The typical synthesis process and characterization are shown in the supporting information section.

Acknowledgements

This work was supported by the Ministry of Science and Technology of Taiwan (Contract Nos. MOST 104-2113-M-002-012-MY3 and MOST 104-2923-M-002-007-MY3) and National Center for Research and Development Poland Grant (No. PL-TW2/8/2015). Y Jin thanks the National Nature Science Foundation of China (No. 11104366), Chongqing Research Program of Basic Research and Frontier Technology (No. cstc2014jcyjA50018), and the Scientific and Technological Research Program of Chongqing Municipal Education Commission (No. KJ1500913). T. Lesniewski would like to acknowledge the support of University of Gdansk Research Grant 538-5200-B468-17. M.G. Brik thanks the supports from the Recruitment Program of High-end Foreign Experts (Grant No. GDW20145200225), the Programme for Foreign Experts offered by Chongqing University of Posts and Telecommunications, Ministry of Education and Research of Estonia, Project PUT430, and European Regional Development Fund (TK141). The calculations were performed using resources provided by Wroclaw Centre for Networking and Supercomputing (http://wcss.pl) under Grant No. WCSS#10117290.

Received: ((will be filled in by the editorial staff))
Published online on ((will be filled in by the editorial staff))

Keywords:narrow-band-emitting•red fluoride phosphor•white light emitting diodes•zero-phonon line•backlighting

[1] R. J. Xie, N. Hirosaki, X. J. Liu, T. Takeda, H. L. Li, *Appl. Phys. Lett.* **2008**, *92*, 201905.
[2] P. Pust, P. J. Schmidt, W. Schnick, *Nat. Mater.* **2015**, *14*, 454-458.
[3] Z. Xia, Q. Liu, *Prog. Mater Sci.* **2016**, *84*, 59-117.
[4] K. Uheda, N. Hirosaki, Y. Yamamoto, A. Naito, T. Nakajima, H. Yamamoto, *Electrochem. Solid-State Lett.* **2006**, *9*, H22-H25.
[5] Y. Arai, S. Adachi, *J. Lumin.* **2011**, *131*, 2652-2660.
[6] M. G. Brik, A. M. Srivastava, *J. Lumin.* **2013**, *133*, 69-72.
[7] H. Zhu, C. C. Lin, W. Luo, S. Shu, Z. Liu, Y. Liu, J. Kong, E. Ma, Y. Cao, R. S. Liu, *Nat. Commun.* **2014**, *5*.
[8] J. H. Oh, Y. J. Eo, H. C. Yoon, Y.-D. Huh, Y. R. Do, *J. Mater. Chem. C* **2016**, *4*, 8326-8348.
[9] Y. K. Xu, S. Adachi, *J. Electrochem. Soc.* **2011**, *158*, J58-J65.
[10] A. M. Srivastava, M. G. Brik, S. J. Camardello, H. A. Comanzo, F. Garcia-Santamaria, *Z. Naturforsch. B* **2014**, *69*, 141-149.
[11] M. Brik, A. Srivastava, *Opt. Mater.* **2016**, *54*, 245-251.
[12] R. Kasa, S. Adachi, *J. Electrochem. Soc.* **2012**, *159*, J89-J95.
[13] J. S. Liao, L. L. Nie, L. F. Zhong, Q. J. Gu, Q. Wang, *Luminescence* **2016**, *31*, 802-807.
[14] L. Huang, Y. W. Zhu, X. J. Zhang, R. Zou, F. J. Pan, J. Wang, M. M. Wu, *Chem. Mater.* **2016**, *28*, 1495-1502.
[15] T. Lesniewski, S. Mahlik, M. Grinberg, R. S. Liu, *Phys. Chem. Chem. Phys.* **2017**, *19*, 32505-32513.

10.1002/anie.201708814

Narrow-band-emitting red phosphor

Control of Luminescence via Tuning of Crystal Symmetry and Local Structure in Mn^{4+}-Activated Narrow Band Fluoride Phosphors **Page – Page**

*Mu-Huai Fang,[⊥] Wei-Lun Wu,[⊥] Ye Jin, Tadeusz Lesniewski, Sebastian Mahlik, Marek Grinberg, Mikhail G. Brik, Alok M. Srivastava, Chang-Yang Chiang, Wuzong Zhou, Donghyuk Jeong, Sun Hee Kim, Grzegorz Leniec, Slawomir M. Kaczmarek, Hwo-Shuenn Sheu, and Ru-Shi Liu**

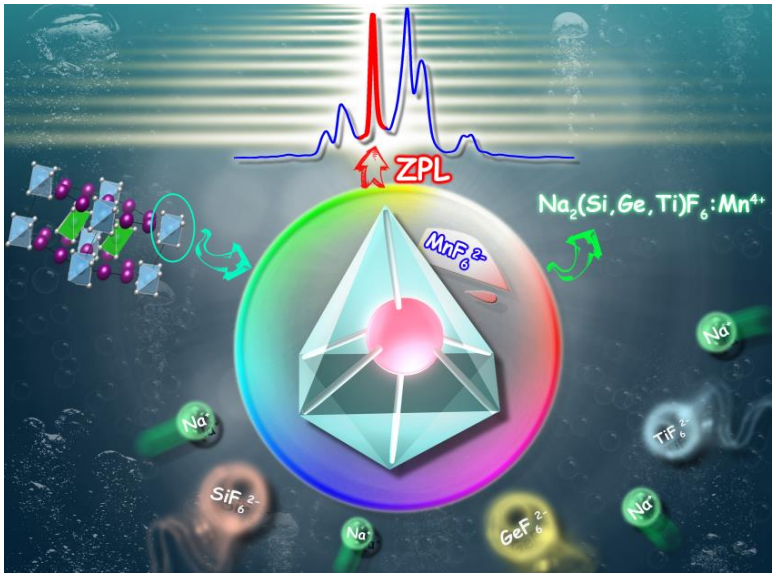

Control of Luminescence via Tuning of Crystal Symmetry and Local Structure in Mn^{4+}-Activated Narrow Band Fluoride Phosphors：In this study, solid solutions of $Na_2(Si_xGe_{1-x})F_6:Mn^{4+}$ and $Na_2(Ge_yTi_{1-y})F_6:Mn^{4+}$ have been successfully synthesized by the co-precipitation method to elucidate the behavior of zero-phonon line (ZPL) in different structure sowing to its high sensitivity to the local coordinated environment. The structures of the products are carefully checked by X-ray diffraction and Rietveld refinement. Interestingly, the ratio between ZPL and the highest emission intensity υ_6 phonon sideband exhibits a strong relationship with luminescent decay rate. First-principles calculations are used to model the variation in the structural and electronic properties of the prepared solid solutions as a function of the composition. The calculated results show good agreement with the experimentally determined structural parameters. To compensate for the limitations of Rietveld refinement, electron paramagnetic resonance is used to prove the diverse local environment for Mn^{4+} in the structure. It also indicates the presence of at least two different positions of Mn^{4+} ions at high and low local symmetry. Moreover, high-resolution steady-state emission spectra are conducted at 10 K to analyze the fine luminescent properties. Finally, the spectral luminous efficacy of radiation (LER) is used to demonstrate that the phosphors with ZPL are provided with higher potential in the practical application.